BIOLOGICAL
CRYSTALLOGRAPHY

Volume 70 (2014)

Supporting information for article:

β-Arm flexibility of HU from *Staphylococcus aureus* dictates a DNA binding and recognition mechanism

Do-Hee Kim, Hookang Im, Jun-Goo Jee, Sun-Bok Jang, Hye-Jin Yoon, Ae-Ran Kwon, Sung-Min Kang and Bong-Jin Lee

S1. The dimerization interface of apo SHU

The dimer interface of SHU has distinct features in its formation that are common in HU homologs. The dimerization of SHU buries 25.9% of the solvent accessible surface area (1890 Å) per HU monomer, which is essentially unchanged by binding with DNA. The aromatic and aliphatic residues located at α1, α2, β1, β2, β5, and α3 stabilize the extensive dimerization interface. The residues not only fill the inner side of the α-helical body but also pack the interspace of the inner strands of dyad-related β-sheets, which cover the α-helical body. Fig. S1*a* demonstrates the hydrophobic residues that contribute to SHU dimerization. The aromatic hydrophobic core especially forms under the saddle-like β-sheets (Fig. S1*b*). The network composed of Phe residues, Phe29 (α2)-Phe47′ (β2), Phe47 (β2)-Phe50′ (β2), and Phe50 (β2)-Phe79′ (β5), which engage in intermolecular interactions, primarily contributes to the stability of SHU (Burley & Petsko, 1985). (The residues in another monomer are denoted with primed numbers.) This aromatic hydrophobic core is a common feature in the HU family; however, Phe29 is particularly conserved in mesophiles, such as *B. stearothermophilus* and *Bacillus subtilis* (White *et al*., 1999). SHU also includes Phe29, which interacts with Phe47′ between the inter-monomer α-helix and β-sheet. These additional aromatic interactions may contribute to maintaining the biological homodimer.

The N-terminus of one monomer and strand β1 of the other monomer form a network of hydrogen bonds that stabilizes dimerization. The amide backbone nitrogen of Gln43 forms hydrogen bonds with the carbonyl backbone oxygen of Met1 in the other monomer. The amide backbone nitrogens of Met1 and Lys3 of the N-terminus form hydrogen bonds with the carbonyl backbone oxygens of Lys41 and Gln43 of strand β1 in the other monomer, respectively. The detailed interactions are shown in Fig. S1*c*. These interfaces and interactions are maintained in the SHU-DNA complex.

S2. Comparison of the interaction of SHU-DNA with that of other protein-DNA complexes

The overall structure of DNA-bound SHU is extremely similar to the DNA complex structures of AHU (PDB code 1P71, RMSD 0.61 Å over aligned Cα atoms and 52% sequence identity) and *E. coli* IHF (PDB code 1IHF, RMSD 1.15 Å over aligned Cα atoms and 39% sequence identity for the α subunit, 40% for the β subunit). A large α-helical body from which two β-ribbon arms embrace the DNA minor groove is observed, and the conserved Pro residues at the end of each arm intercalate between base pairs, creating and/or stabilizing two DNA kinks. The overall interactions of SHU with TR3 are similar to the interactions of AHU. The SHU protein in the SHU-DNA complex shows similar structural features to the IHF and AHU proteins in the IHF-DNA and AHU-DNA complexes, respectively. Furthermore, as previously shown in the structure of IHF/HU-DNA, neighbouring SHU-

DNA complexes pack end-to-end, forming a pseudocontinuous helix. The overall structure of SHU also shares similarities with other protein-DNA structures (Fig. S2*b*).

The β-ribbon arms wrap around the minor DNA groove of the DNA, and at the tip of each arm, the conserved Pro residues intercalate between base pairs, creating and/or stabilizing two DNAs. When the two DNA complex structures of SHU and AHU were superimposed, the overall structures fit well. As observed in apo homologs, the rigid α-helical body is well overlaid; however, the β-ribbon arms of SHU are bent toward DNA compared with those of AHU. Furthermore, the DNA of the SHU-DNA complex structure is over-twisted compared with the DNA of AHU.

Detailed structural differences arise from Arg61-DNA interaction. TR3 has an unpaired T7 flipped out of the duplex on each strand. In the AHU-DNA complex, the 5′ phosphate of the unpaired T7 forms a bidentate hydrogen bond with the Arg61 side chain of the neighbouring complex (Fig. S3*a*). IHF also exhibits a similar interaction at a conserved Arg residue (Arg63). In the SHU-DNA complex, the Glu40 side chain (OE2) (chain A) of the neighbouring complex forms a hydrogen bond with N3 of the flipped T7 (chain C), and the Arg61 side chain lies along the DNA. The side chain does not form a hydrogen bond with the 5′ phosphate of the flipped out T7 of the neighbouring complex (Fig. S3*b*). The flipped T7 (chain D) O4 forms a hydrogen bond with the neighbouring Asn62 ND2 (chain A) (Fig. S3*b*). The asymmetric composition and crystal packing of apo SHU may result in the differences in SHU binding properties compared with AHU and IHF. In the SHU-DNA complex, we can observe inward bending of the SHU β-arms compared with AHU. This bending could be explained by the twist angle and crystal packing force. At the C-terminal region of chain B of the SHU-DNA complex, the longer DNA binding site and small dihedral angle may account for this sharper bending. These differences between SHU and its homologs suggest the flexible DNA bending property and the architectural roles of HU.

Table S1 Oligonucleotides used in mutagenesis.

Mutants	Oligomer
R55A FOR	5'-GAG GTA CGT GAA GCA GCT GCA CGT AAA G-3'
R55A REV	CTT TAC GTG CAG CTG CTT CAC GTA CCT C
R58A FOR	GTG AAC GTG CTG CAG CAA AAG GTC GTA ACC C
R58A REV	GGG TTA CGA CCT TTT GCT GCA GCA CGT TCA C
K59A FOR	CGT GCT GCA CGT GCA GGT CGT AAC CCT C
K59A REV	GAG GGT TAC GAC CTG CAC GTG CAG CAC G
R61A FOR	GCTGCACGTAAAGGTGCTAACCCTCAAACTGG
R61A REV	CCAGTTTGAGGGTTAGCACCTTTACGTGCAGC
P63A FOR	CGTAAAGGTCGTAACGCTCAAACTGGTAAAG
P63A REV	CTTTACCAGTTTGAGCGTTACGACCTTTACG

Table S2 Overall structural comparison of apo SHU and SHU-HU homologs.

	Species (sequence identity %)	RMSD on Ca atoms (Å)
Apo chain B/D[a]		0.25 for 68 C_α atoms
Apo chain AC/BC		0.56 for 148 C_α atoms
SHU/1B8Z[b]	*T. maritima* (58%)	0.63 for 114 C_α atoms
SHU/1WTU	*B. phage* SPO1 (40%)	2.58 for 132 C_α atoms
SHU/4DKY	*M. tuberculosis* (39%)	0.80 for 142 C_α atoms (chain A[c])
SHU/3RHI	*B. anthracis* (71%)	0.74 for 125 C_α atoms (chain A/B) 0.73 for 126 C_α atoms (chain C/D)
SHU/1HUE,1HUU	*B. stearothermophilus* (80%)	1.05 (1HUE) for 135 C_α atoms, 0.35 (1HUU) for 124 C_α atoms
SHU/2O97	*E. coli* (α: 59%, β: 62%)	0.46 for 128 C_α atoms

[a] Chains A, B, C, and D represent the monomer chain in the asymmetric unit of apo SHU.

[b] The homologs names are represented with PDB codes.

[c] The chains in parentheses were selected for RMSD calculations.

Table S3 Oligomers used as DNA substrates in EMSA and ITC analyses.

	DNA sequence	Remarks
1	5’ TGCTTATCAATTTGTTGCACC ACGAATAGTTAAACAACGTGG	Completely complementary
2	5’ TGCTTATCAATTTGTTGCACC[a] ACGT-T-GTTAAACAACGTGG	Partially unpaired
3	5’ TTGTGCATGCTTATCAATTTG-T-TGCATGCACAA AACACGTACGT-T-GTTTAACTATTCGTACGTGTT	Extended TR3
4	5’ TGCTTATCAATTTGTTGCACC ACGT-T-GTTT	Partially complementary
5	5’ TGCTACAATTTGTTGCACC CCACGTTGTTTAACATCGT	Unpaired T5 and T7 are removed
6	5’ TGCTTATCAATTTG-T-TGCACC CCACGT-T-GTTTAACTATTCGT	TR3
7	5’ TGCTTACAATTTGT-TGCACC CCACGT-TGTTTAACATTCGT	Unpaired T7 are removed
8	5’ TGCTTATCAATTTG-T-TGCACC CCACGT-T-GTTAAACTATTCGT	AT rich
9	5’ TGCTTATCAGCGTG-T-TGCACC CCACGT-T-GTCGCACTATTCGT	GC rich
10	5’ TTATCAATTTGTTGC AATAGTTAAACAACG	15mer TR3
11	5’ TTGCACCTGCTTATCAATTTGTTGCACCTGCTTAT AACGTGGACGAATAGTTAAACAACGTGGACGAATA	35mer TR3

[a] Pink: mismatched, Blue: unpaired but stacked, Green: unpaired and flipped. Specific nucleotides are underlined.

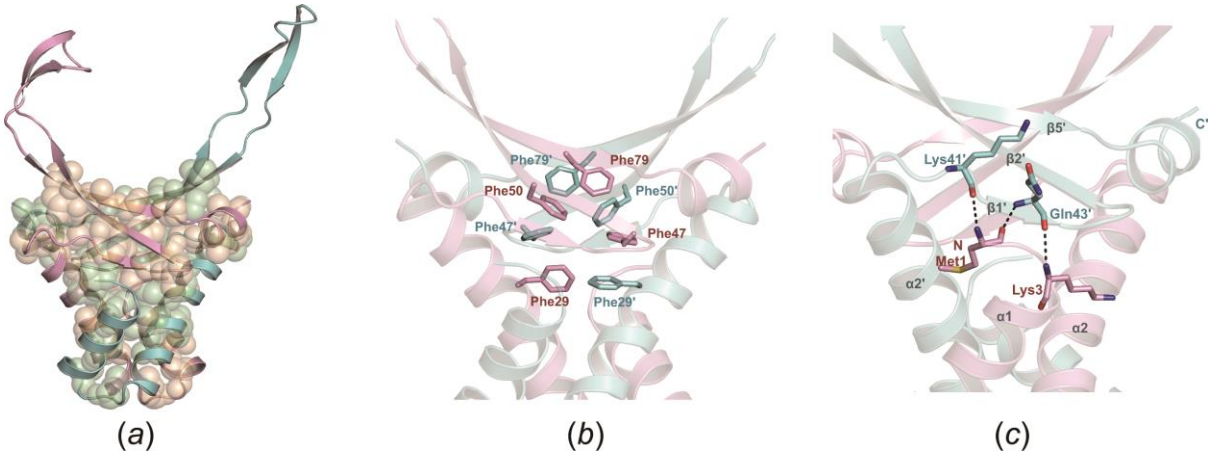

Figure S1 Dimerization interface of apo SHU and the major characteristic interactions within the dimerization interface. (*a*) The hydrophobic core of the interface. The hydrophobic residues in the dimer interface are represented as light yellow (chain B) and light green (chain D) transparent spheres. (*b*) Phe residues in the hydrophobic cores. The Phe residues in SHU are positioned in the interior of the dimer. The network of Phe residues Phe29 (α2)-Phe47′(β2), Phe47 (β2)-Phe50′(β2), and Phe50 (β2)-Phe79′ (β5) with inter-monomer interactions is a common feature in the HU family; however, Phe29 is particularly conserved in HU mesophiles. (*c*) The interactions at the N-terminus (chain B) attach α1 to β1' at the interface of each monomer. (Because the interactions of chain D are identical to those of chain B, only the interactions of chain B are shown.) The atoms involved in hydrogen bonding contribute to the stability of the interface and are shown in red for oxygen and blue for nitrogen. The hydrogen bonds are represented by black dashed lines.

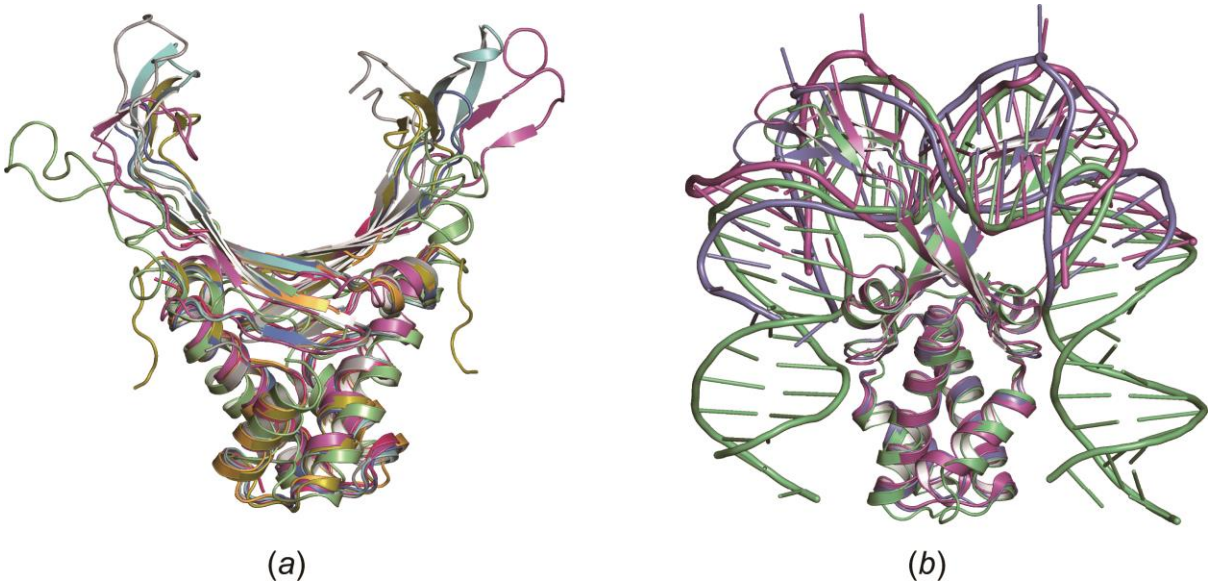

(*a*) (*b*)

Figure S2 Comparison of SHU with homologs. (*a*) Superimposition of homolog structures on apo SHU (cyan). The superimposition shows that the β-arms are flexible compared with the α-helical body. The other structures are *B. stearothermophilus* HU (X-ray, PDB code 1HUU, blue/ NMR, PDB code 1HUE, plum), *B. anthracis* HU (X-ray, PDB code 3RHI, gray), *E. coli* HU (X-ray, PDB code 2O97, hot pink), *T. maritima* HU (X-ray, PDB code 1B8Z, orange), *M. tuberculosis* HU (X-ray, PDB code 4DKY, yellow), and *B. phage* SPO1 TF1 (NMR, PDB code 1WTU, green). (*b*) Superimposition of the SHU-DNA (X-ray, plum), IHF-DNA (X-ray, PDB code 1IHF, green), and AHU-DNA (X-ray, PDB code 1P71, purple) structures.

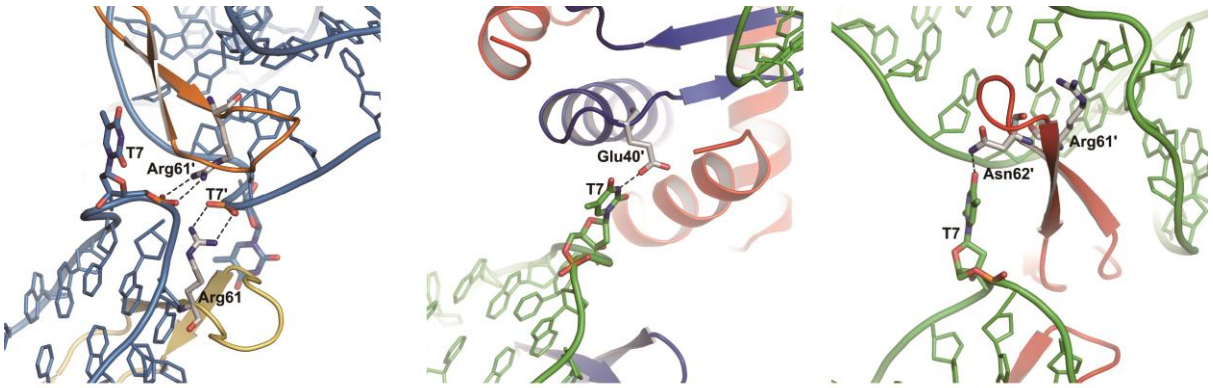

(*a*) (*b*)

Figure S3 The structural differences between SHU-DNA and AHU-DNA in the region of the flipped T7. (*a*) Interactions in AHU-DNA. Arg61 in AHU interacts with the 5' phosphate of the flipped out T7 of a neighbouring complex through bidentate hydrogen bonding. (*b*) Interactions in SHU-DNA. Hydrogen bonds are formed between the flipped out T7 and neighbouring SHU. Glu40 in chain B (left) and Asn62 in chain A (right) form hydrogen bonds with the N3 and O4 of the flipped out T7, respectively.

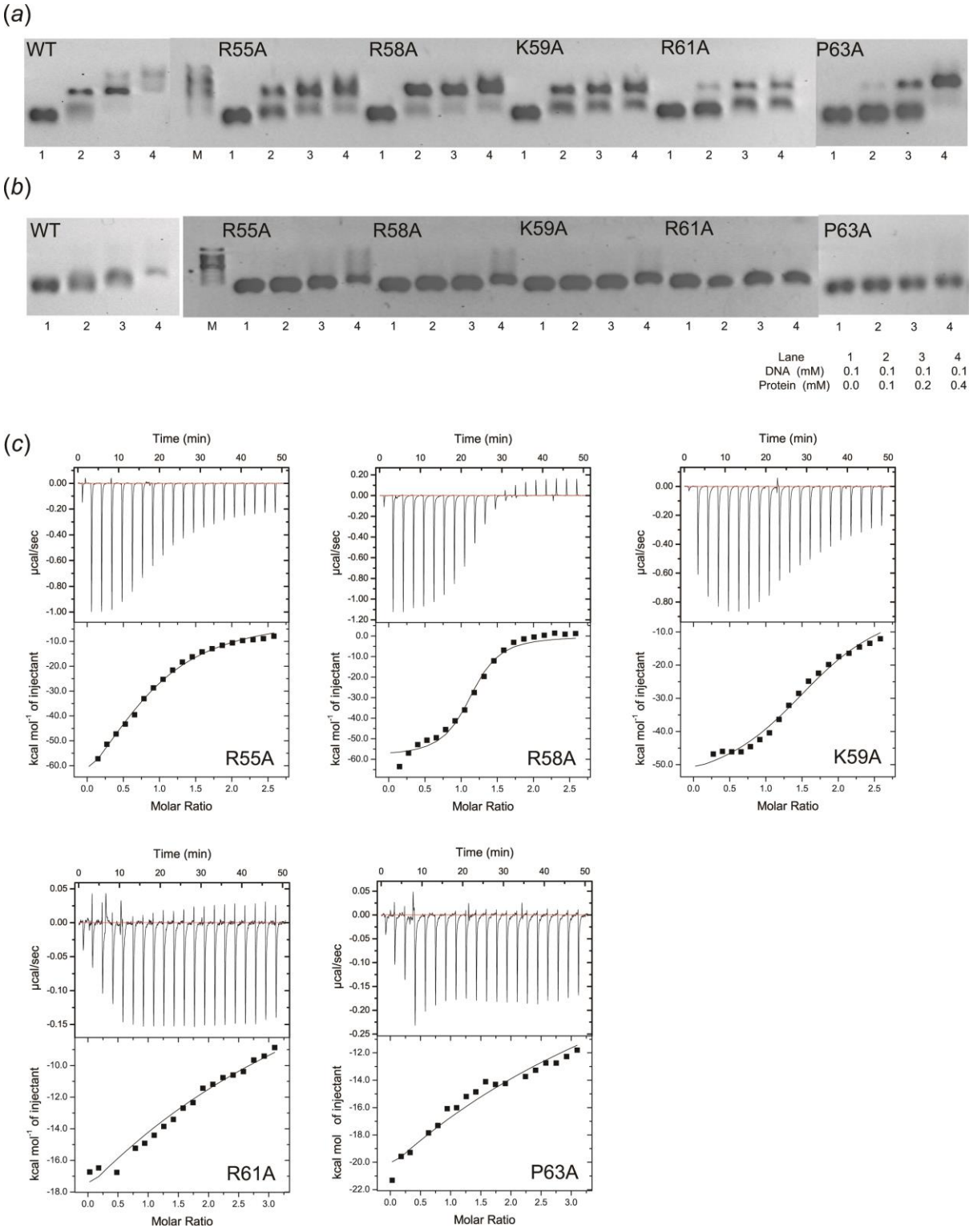

Figure S4 DNA binding properties as determined from EMSA and ITC experiments. (*a*) Electrophoretic mobility shift assay. WT SHU and five SHU mutants at various concentrations were mixed with 0.05 mM dsDNA No. 2 (*a*) and No. 6 (*b*). The detailed protein and DNA concentrations are indicated according to lane number. Free and bound DNAs were separated on an 0.8% agarose gel, as described in the Materials and methods and in Fig. 5. (*c*) ITC experiments of SHU muntants

binding to No. 6 oligomer (TR3). R61A and P63A showed reduced DNA binding properties, and R55A and K59A also exhibited reduced affinities for TR3 compared to that for WT SHU (reference Table. 2). R58A demonstrated a small change in affinity (represented with K_d). These ITC results coincide with the EMSA results.

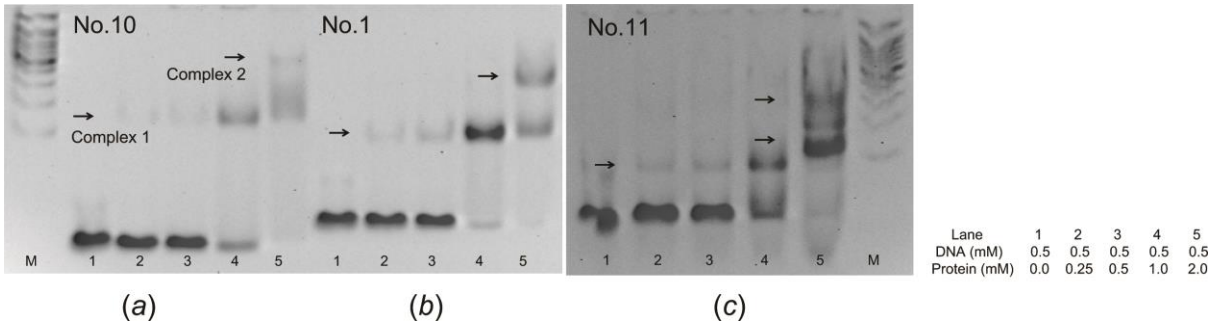

Figure S5 Size of the SHU binding site. Titrations of SHU with various lengths of DNA ((*a*) 15-mer, (*b*) 21-mer, and (*c*) 35-mer) by symmetrically shortening or increasing the TR3 at both ends (the DNA sequences are shown in Table S3). The detailed protein and DNA concentrations are indicated according to lane number. The detailed assay condition is identical to the one in Fig. 5.

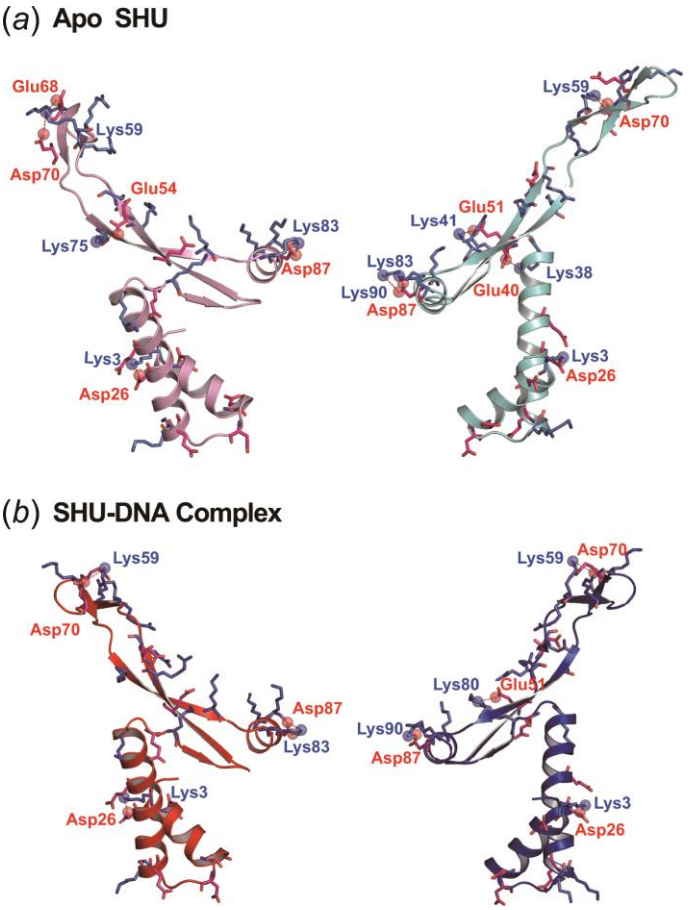

Figure S6 Salt bridges in (*a*) apo SHU and (*b*) the SHU-DNA complex. We used the ESBRI server (a web server for evaluating salt bridges in proteins) (Costantini *et al.*, 2008) to find salt bridges within 4 Å in apo SHU and SHU-DNA complex structures. SHU possesses 31% charged residues, which are shown in stick representation. The basic residues, Lys and Arg, and the acidic residues, Glu and Asp, are shown with light blue and plum, respectively. The red dashes denote salt bridges, and the atoms involved in the interaction are represented as spheres. The Lys3-Asp26, Lys59-Asp70, Lys83-Asp87, and Lys90-Asp87 salt bridges are maintained when SHU binds to the DNA, while the Lys80-Glu51 salt bridge is newly formed.

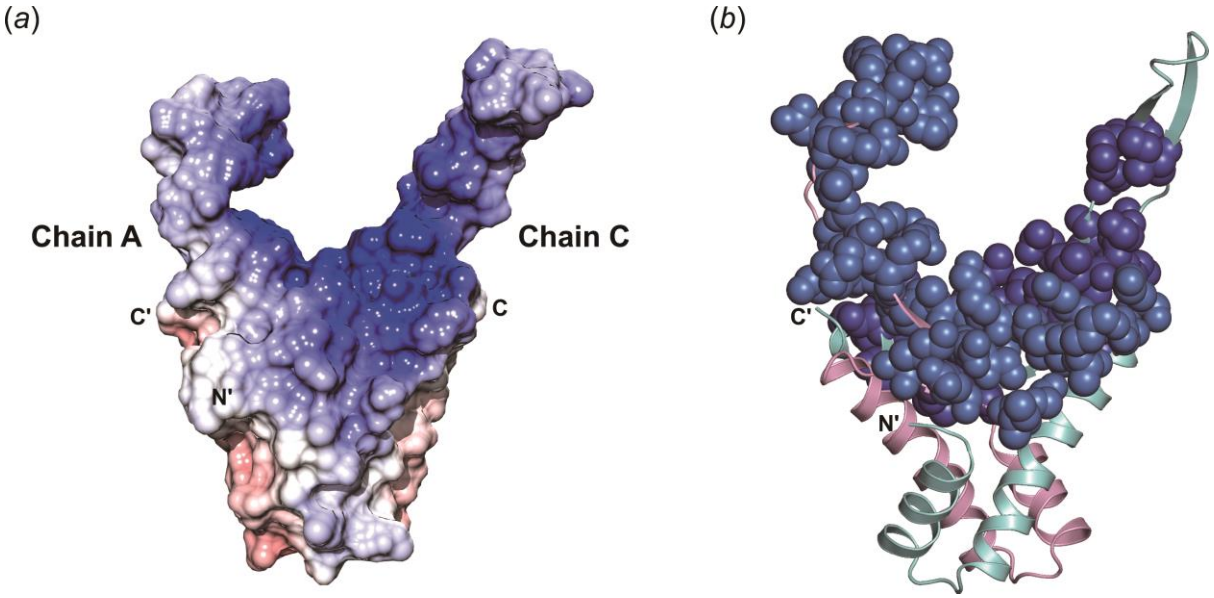

Figure S7 Predicted DNA binding site. (*a*) Electrostatic surface representation of apo SHU. The positive and negative potentials are blue and red, respectively. The large positive strip is presented on the surface; however, the positive strip is not connected fully at the N-terminus. (*b*) The DNA binding sites predicted by the PFP web server for apo SHU. The protein is shown in ribbon representation, and the residues predicted to bind DNA are shown in sphere representation with blue. The large positive electrostatic patch on a protein surface corresponds well to the residues that are involved in DNA binding.

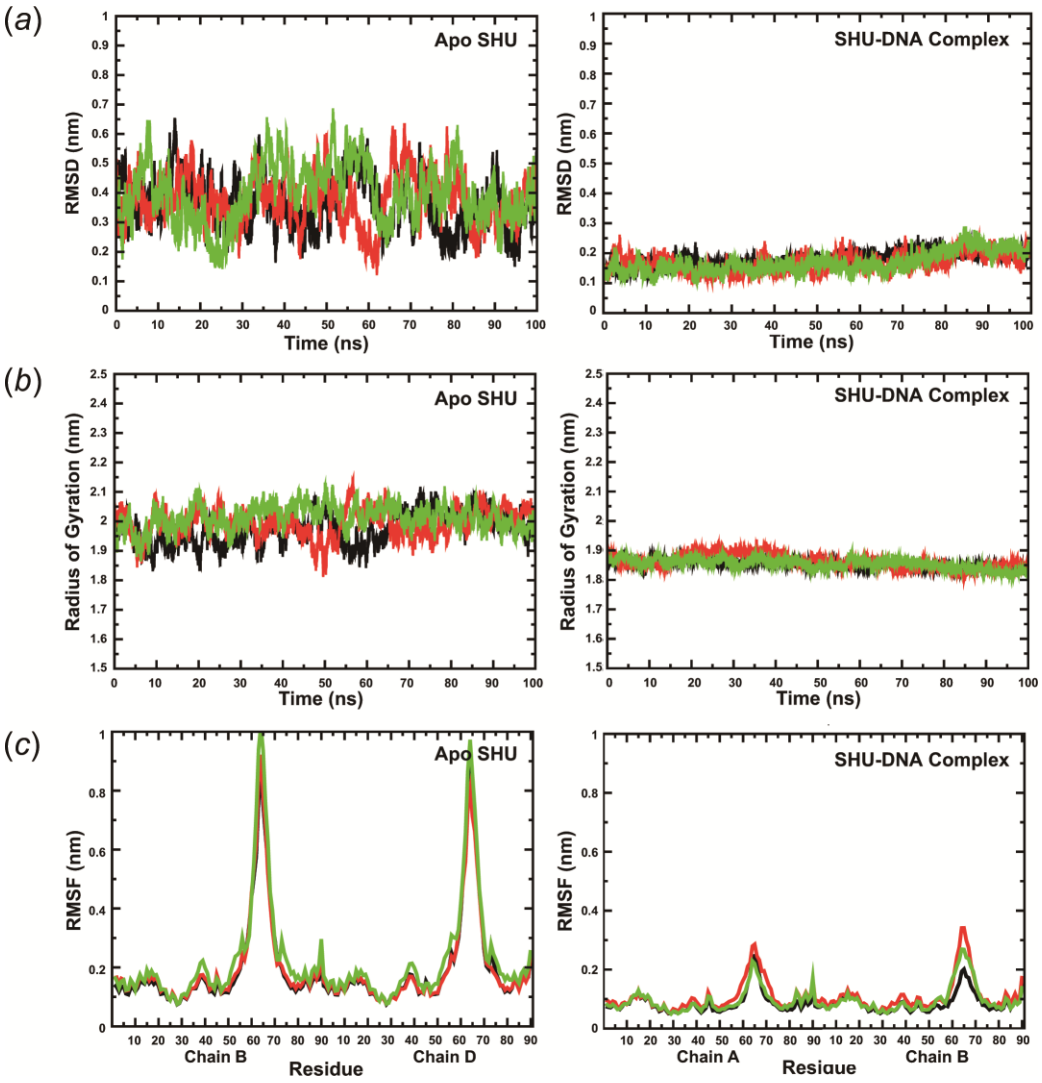

Figure S8 Structural dynamics of SHU. (*a*) RMSD, (*b*) Rg, and (*c*) RMSF of apo SHU and the SHU-DNA complex. The molecular dynamics simulations for 100 ns of apo SHU and the SHU-DNA complex were repeated three times each. RMSD and Rg values indicate that apo SHU is more stable than the SHU-DNA complex during the MD simulation. The residues that show large deviations in the RMSF analysis coincide with the bending region from the DynDom analysis. The degree of deviation is smaller in the SHU-DNA complex than in apo SHU.

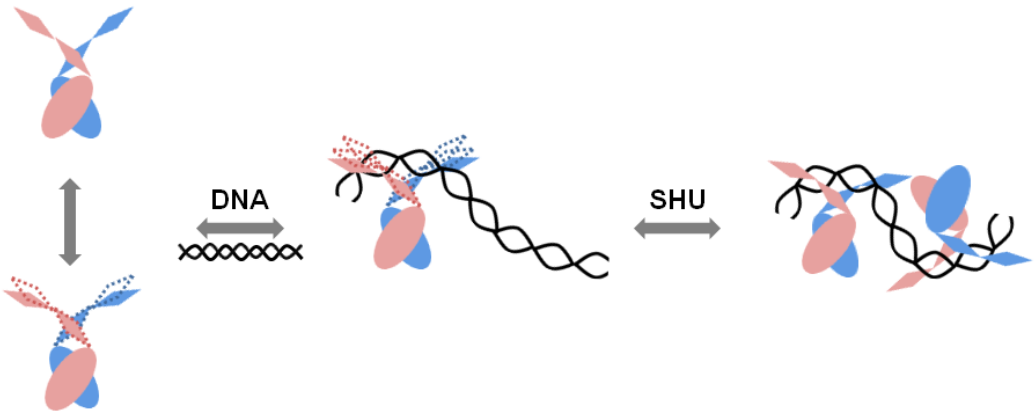

Figure S9 Suggested DNA binding mechanism of SHU. The β-arms of the SHU dimer and DNA exist in dynamic conformational states and DNA exists as various bent states according to their environment. The flexible nature of the β-arm contributes to the diverse biological roles of SHU in DNA architecture. SHU binds to DNAs without sequence-specificity but preferentially recognizes distorted DNA, and binds it by utilizing energetically favoured residues lining the β-arms. At high concentrations of SHU, additional SHU binds to pre-existing SHU-DNA complex, forming higher-order complex states with 7-11 bp binding site sizes. This binding alludes to its role of DNA compaction.